Biochemical and Biophysical Research Communications 457 (2015) 451–456

Contents lists available at ScienceDirect

Biochemical and Biophysical Research Communications

journal homepage: www.elsevier.com/locate/ybbrc

Bcl6 promotes osteoblastogenesis through Stat1 inhibition

Atsuhiro Fujie [a], Atsushi Funayama [a], Yoshiteru Miyauchi [a], Yuiko Sato [a, b], Tami Kobayashi [a, d], Hiroya Kanagawa [a], Eri Katsuyama [a], Wu Hao [a], Toshimi Tando [a], Ryuichi Watanabe [a], Mayu Morita [c], Kana Miyamoto [a], Arihiko Kanaji [a], Hideo Morioka [a], Morio Matsumoto [a], Yoshiaki Toyama [a], Takeshi Miyamoto [a, d, *]

[a] Department of Orthopedic Surgery, Keio University School of Medicine, 35 Shinano-machi, Shinjuku-ku, Tokyo 160-8582, Japan
[b] Department of Musculoskeletal Reconstruction and Regeneration Surgery, Keio University School of Medicine, 35 Shinano-machi, Shinjuku-ku, Tokyo 160-8582, Japan
[c] Department of Dentistry and Oral Surgery, Keio University School of Medicine, 35 Shinano-machi, Shinjuku-ku, Tokyo 160-8582, Japan
[d] Department of Integrated Bone Metabolism and Immunology, Keio University School of Medicine, 35 Shinano-machi, Shinjuku-ku, Tokyo 160-8582, Japan

ARTICLE INFO

Article history:
Received 26 December 2014
Available online 15 January 2015

Keywords:
Osteoblast
Differentiation
Bone
Bcl6
Stat1

ABSTRACT

Bone mass is tightly controlled by a balance between osteoclast and osteoblast activities. Although these cell types mature via different pathways, some factors reportedly regulate differentiation of both. Here, in a search for factors governing osteoblastogenesis but also expressed in osteoclasts to control both cell types by one molecule, we identified B cell lymphoma 6 (Bcl6) as one of those factors and show that it promotes osteoblast differentiation. Bcl6 was previously shown to negatively regulate osteoclastogenesis. We report that lack of Bcl6 results in significant inhibition of osteoblastogensis *in vivo* and *in vitro* and in defects in secondary ossification center formation *in vivo*. Signal transducer and activator of transcription 1 (Stat1) reportedly attenuates osteoblast differentiation by inhibiting nuclear translocation of runt-related transcription factor 2 (Runx2), which is essential for osteoblast differentiation. We found that lack of Bcl6 resulted in significant elevation of Stat1 mRNA and protein expression in osteoblasts and showed that Stat1 is a direct target of Bcl6 using a chromatin immune-precipitation assay. Mice lacking both Bcl6 and Stat1 (DKO) exhibited significant rescue of bone mass and osteoblastic parameters as well as partial rescue of secondary ossification center formation compared with Bcl6-deficient mice *in vivo*. Altered osteoblastogenesis in Bcl6-deficient cells was also restored in DKO *in vitro*. Thus, Bcl6 plays crucial roles in regulating both osteoblast activation and osteoclast inhibition.
© 2015 Elsevier Inc. All rights reserved.

1. Introduction

Bone homeostasis is regulated cooperatively by bone-forming osteoblasts and bone-resorbing osteoclasts, and such activity is termed coupling [1–3]. To date, several transcription factors essential for either osteoblast or osteoclast differentiation have been identified. Runt-related transcription factor 2 (Runx2) and Sp7 were both identified as essential for osteoblastogenesis, and both Runx2- or Sp7-deficient mice exhibit complete abrogation of bone formation [4–6]. Likewise, c-Fos and nuclear factor of activated T cells 1 (NFATc1) were both found to be essential for osteoclast differentiation, and lack of either c-Fos or NFATc1 resulted in failure of osteoclastogenesis [7,8]. Sp7 reportedly acts downstream of Runx2 in osteoblasts [6], while NFATc1 was shown to be a c-Fos target in osteoclasts [7,9]. B cell lymphoma 6 (Bcl6) is a transcriptional repressor so named because it was identified as a transcript in B cell lymphoma cells [10,11]. Previously, we demonstrated that Bcl6 inhibits osteoclast differentiation by attenuating transcription of osteoclastic genes, such as *NFATc1* [12]. Signal transducer and activator of transcription 1 (Stat1) has been shown to inhibit osteoblastogenesis by interacting with Runx2 and blocking its nuclear translocation [13]. However, how Stat1 expression is regulated in osteoblasts is not known.

To date, various molecules including Semaphorin 3A [14], Zfp521-Ebf1 [15], DC-STAMP [16], and Atp6v0d2 [17] have all been shown to regulate both osteoblasts and osteoclasts by expressed in each cell type or through regulation of osteoclast activity, and all

* Correspondence author. Department of Orthopedic Surgery, Keio University School of Medicine, 35 Shinano-machi, Shinjuku-ku, Tokyo 160-8582, Japan. Fax: +81 3 3353 6597.
E-mail address: miyamoto@z5.keio.jp (T. Miyamoto).

http://dx.doi.org/10.1016/j.bbrc.2015.01.012
0006-291X/© 2015 Elsevier Inc. All rights reserved.

are considered therapeutic targets in strategies to increase bone mass.

Here, we found that Bcl6 is expressed in osteoblasts and demonstrate that it regulates osteoblastogenesis through Stat1 inhibition. Bcl6-deficient mice exhibited significant reduction of bone mass and attenuated osteoblast differentiation with significant elevation of Stat1 expression in osteoblasts.

2. Materials and methods

2.1. Mice

C57BL/6 background wild-type mice were purchased from Sankyo Labo Service (Tokyo, Japan). *Bcl6*$^{-/-}$ and *Stat1*$^{-/-}$ mice were established as previously described [18,19], Bcl6 KO, Bcl6-Stat1 DKO, and control littermates were injected intraperitoneally with 16 mg/kg calcein (Dojindo Co.) at 6 and 1 days before sacrifice to evaluate bone formation rate, and were necropsied at 6 weeks of age. Hindlimbs were removed, fixed with 70% ethanol, and subjected to DEXA analysis to measure bone mineral density, for micro CT analysis and for bone-histomorphometric analysis, as previously described [12,20]. Animals were maintained under specific pathogen-free conditions in animal facilities certified by the Keio University School of Medicine animal care committee. All animal procedures were approved by the Keio University School of Medicine animal care committee.

2.2. Cell culture

To assess osteoblast formation *in vitro*, primary osteoblasts isolated from newborn mouse calvaria were cultured for 72 h in αMEM (Sigma–Aldrich Co., St. Louis, MO, USA) containing 10% heat-inactivated fetal bovine serum (FBS, JRH Biosciences Lenexa, KS, USA) supplemented with or without BMP2 (300 ng/ml, PeproTech Ltd., Rocky Hill, NJ, USA) for three days. Osteoblastogenesis was evaluated by Alp staining and realtime or RT PCR analysis. For osteoclast culture, osteoclast progenitor cells were isolated from mouse BM cells and cultured in the presence of M-CSF (50 ng/ml) and recombinant soluble RANKL (25 ng/ml, PeproTech Ltd., Rocky Hill, NJ, USA) as described [12,20].

For realtime PCR, total RNA was isolated from cultured cells using an RNeasy mini kit (Qiagen), and cDNA was synthesized using oligo (dT) primers and reverse transcriptase (Wako Pure Chemicals Industries). Quantitative PCR was performed using SYBR Premix ExTaq II reagent and a DICE Thermal cycler (Takara Bio Inc., Shiga, Japan), and results were quantified using the ddCt method. *β-actin* (*Actb*) expression served as an internal control. Primers for *Bcl6*, *Alp*, *Col1a1*, *Sp7* and *Actb* were as follows.

Bcl6-forward: 5′-AGACGCACAGTGACAAACCATACA-3′
Bcl6-reverse: 5′-CTCCACAAATGTTACAGCGATAGG-3′
Alp-forward: 5′-CACCATTTTTAGTACTGGCCATCG-3′
Alp-reverse: 5′-GCTACATTGGTGTTGAGCTTTGG-3′
Col1a1-forward: 5′-CATGTTCAGCTTTGTGGACCTC-3′
Col1a1-reverse: 5′-CCTTAGGCCATTGTGTATGCAG-3′
Sp7-forward: 5′-GATGGCGTCCTCTCTGCTTG-3′
Sp7-reverse: 5′-AGGGCTAGAGCCGCCAAAT-3′
β-actin-forward: 5′-TGAGAGGGAAATCGTGCGTGAC-3′
β-actin-reverse: 5′-AAGAAGGAAGGCTGGAAAAGAG-3′

For western blotting, whole cell lysates were prepared using RIPA buffer (1% Triton X-100, 1% sodium deoxycholate, 0.1% SDS, 150 mM NaCl, 5 mM EDTA, 1 mM dithiothreitol, 10 mM Tris–HCl, pH 7.5) supplemented with a protease inhibitor cocktail (Sigma–Aldrich Co.). Equivalent amounts of protein were separated by SDS-PAGE and transferred to a PVDF membrane (EMD Millipore Corporation). Proteins were detected using anti-Stat1 (Cell Signaling Technology, Inc.) and anti-Actin (Sigma–Aldrich Co., St Louis, MO) antibodies. No bands were detected using the anti-Stat1 antibody in Stat1-deficient cell lysates (data not shown).

For immunohistochemical staining, cultured cells were fixed with 4% paraformaldehyde/PBS for 20 min at room temperature. Subsequently, cells were incubated in 5% BSA-PBS and then stained with rabbit anti-Runx2 antibody (Santa Cruz) followed by alexa488-conjugated goat anti-rabbit Igs' antibody (Invitrogen Corp.). Nuclei were counterstained using DAPI (Chemical Dojin).

2.3. Chromatin immunoprecipitation (ChIP)

ChIP was performed on osteoblastic MC3T3E1 cells using the ChIP-IT Enzymatic Kit (ActivMotif Inc., Carlsbad, CA, USA), according to the manufacturer's instructions. Immunoprecipitation was performed using a rabbit anti-Bcl6 antibody (N-3, Santa Cruz) as described [21]. DNA was purified using a Qiaquick PCR Purification Kit (QIAGEN Inc., Valencia, CA, USA) and analyzed using the following primers: *Stat1* promoter: 5′-GAGTCAGTTCTGTGATGCCTTTG-3′ (sense) and 5′-TCTAAAGAGTGAGTTCCAGGACA-3′ (antisense).

2.4. Statistical analyses

Statistical analyses were performed using an unpaired two-tailed Student's *t*-test and ANOVA ($^{*}P < 0.05$; $^{**}P < 0.01$; $^{***}P < 0.001$; NS, not significant, throughout the paper). All data are expressed as the mean ± SD.

3. Results

3.1. Bcl6 is expressed in osteoblasts and required for osteoblastogenesis

Previously, we reported that Bcl6 negatively regulates osteoclastogenesis [12], however, it was not known whether it functions in osteoblasts. Thus, we analyzed *Bcl6* expression in primary osteoblasts using realtime PCR and found that it is expressed in osteoblasts at levels similar to those seen in osteoclasts (Fig. 1A). As previously reported [12], we found that osteoclastogenesis was activated in Bcl6-deficient mice. However, when we analyzed osteoblastic parameters in Bcl6-deficient mice, we found that osteoblast surface per bone surface (Ob.S/BS) was significantly low in Bcl6-deficient compared with control mice *in vivo* (Fig. 1B). We then isolated osteoblastic cells from Bcl6-deficient and wild-type neonatal calvaria, cultured them with or without bone morphogenetic protein 2 (BMP2) to promote osteoblast differentiation, and evaluated osteoblastogenesis by alkaline phosphatase (Alp) staining (Fig. 1C) and realtime PCR for osteoblastic factors such as *Alp*, *Col1a1* and *Sp7* (Fig. 1D). We found that osteoblast differentiation was inhibited in Bcl6-deficient compared with wild-type cells, as determined by Alp staining (Fig. 1C). Likewise, *Alp*, *Col1a1* and *Sp7* expression was significantly inhibited in Bcl6-deficient compared with wild-type cells (Fig. 1D). In contrast, osteoblastic MC3T3-E1 cells overexpressing Bcl6 exhibited significantly accelerated osteoblast differentiation (Fig. S1), suggesting that Bcl6 regulates osteoblastogenesis.

3.2. Stat1 is negatively regulated by Bcl6 in osteoblasts

Next, we analyzed molecular mechanisms underlying regulation of osteoblastogenesis by Bcl6. To do so, we analyzed activation of Smad 1,5,8, which are required to promote osteoblast

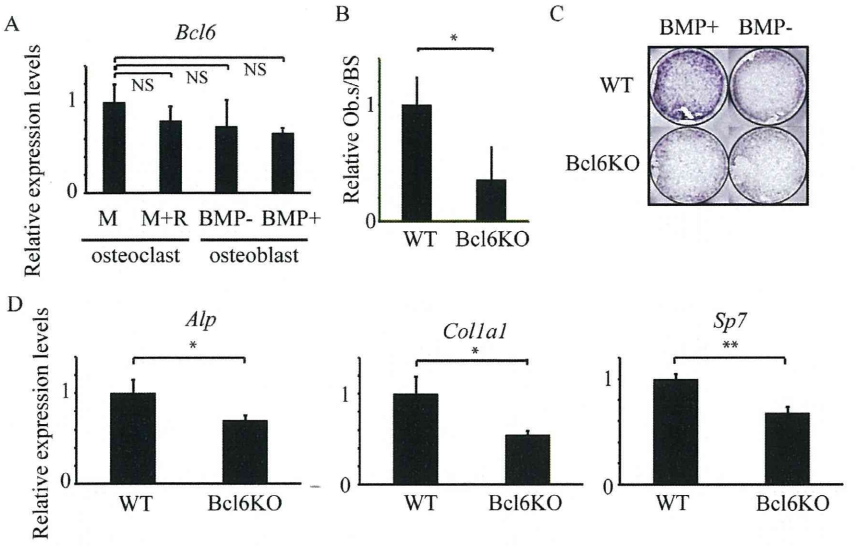

Fig. 1. Bcl6 KO mice exhibit inhibited osteoblastogenesis *in vivo* and *in vitro*. (A) *Bcl6* expression in osteoblasts or osteoclasts was determined by realtime PCR. M, M-CSF alone, M + R, M-CSF plus RANKL. Data represent mean *Bcl6* expression relative to *β-actin* ± SD (NS: not significant, $n = 3$). (B) Bone histomorphometrical analysis of osteoblast surface per bone surface (Ob.S/BS) of tibias from six weeks old wild-type (WT) and Bcl6 KO (KO) female mice. Data are mean relative values ± s.d. of Ob.S/BS. ($^*P < 0.05$, $n = 5$). (C, D) Primary osteoblasts isolated from wild-type (WT) and Bcl6 KO (KO) mice were cultured in the presence or absence of BMP2 (300 ng/ml) for three days, and osteoblastogenesis was evaluated by Alp staining (D) or realtime PCR (E). Data represent means ± s.d of *Alp*/*β-actin*, *Col1a1*/*β-actin* or *Sp7*/*β-actin* levels ($^*P < 0.05$, $^{**}P < 0.01$, $n = 3$). Representative data of two (B) and at least three (A, C and D) independent experiments are shown.

differentiation following BMP2 stimulation, using western blotting of osteoblast lysates [22,23]. We found that Smad 1,5,8 were equivalently phosphorylated in wild-type and Bcl6-deficient osteoblasts following BMP2 treatment (Fig. S2), suggesting that BMP2 signal was transduced to Smads in Bcl6-deficient cells.

Since Bcl6 is a transcriptional repressor, we searched for candidate targets in osteoblasts by screening for molecules that 1) exhibited Bcl6 consensus binding sites in their promoter regions and 2) regulated osteoblast differentiation. Based on these criteria, we identified *Stat1* as a candidate Bcl6 target (Fig. 2A). A Bcl6 consensus binding site located upstream of the *Stat1* gene was conserved between humans and mice (Fig. 2A), and Stat1 reportedly negatively regulates osteoblastogenesis [13]. We then undertook a chromatin immune-precipitation assay in osteoblastic MC3T3E1 cells and found that Bcl6 was recruited to the *Stat1* promoter in osteoblasts (Fig. 2B). Stat1 expression in Bcl6-deficient osteoblasts was significantly higher than that seen in wild-type osteoblasts at both the mRNA and protein levels (Fig. 2C, D). These results suggest that *Stat1* is directly repressed by Bcl6 in osteoblasts.

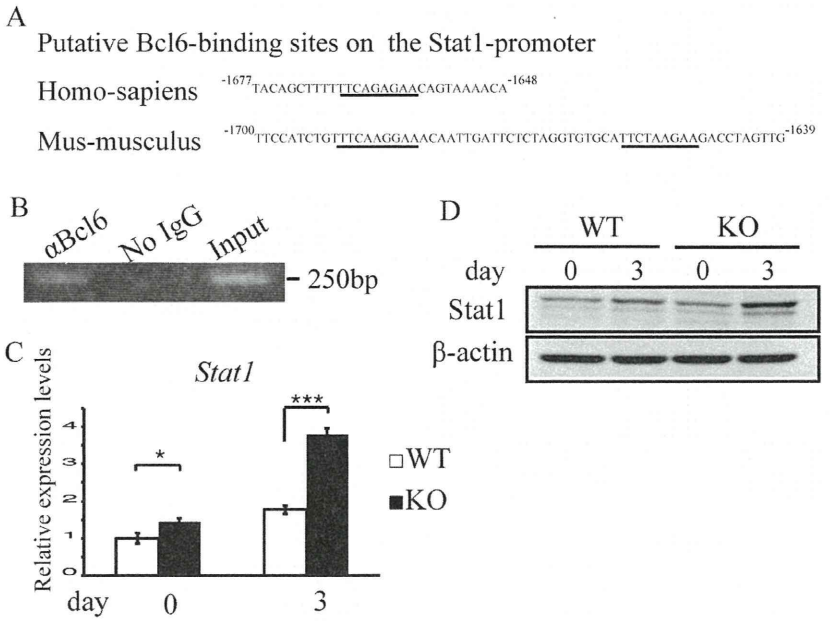

Fig. 2. Stat1 is a direct target of Bcl6 in osteoblasts. (A) Promoter sequence of human and mouse *Stat1* genes. Underlining indicates Bcl6 consensus binding sites. (B) Recruitment of Bcl6 to the *Stat1* promoter was analyzed in MC3T3E1 cells by a ChIP assay. (C, D) Stat1 expression was determined by realtime PCR (C) and western blotting (D). Data represent means ± s.d of *Stat1*/*β-actin* ($^*P < 0.05$, $^{***}P < 0.001$, $n = 3$). Representative data of two (B) and at least three (C, D) independent experiments are shown.

3.3. Stat1 loss rescues reduced bone mass seen in Bcl6-deficient mice

We next asked whether elevated Stat1 expression in Bcl6-deficient osteoblasts might underlie reduced bone mass and altered osteoblastogenesis by generating Bcl6 and Stat1 double mutant mice (DKO). DEXA analysis demonstrated that reduced bone mass seen in Bcl6 single knockout (Bcl6 KO) mice was significantly rescued in DKO mice (Fig. 3A). Altered trabecular bone formation in Bcl6-deficient mice, as assessed by toluidine blue staining and micro CT analysis, was restored in DKO mice (Fig. 3B, C). Bcl6-deficient mice exhibited impaired secondary ossification center formation, an effect partially rescued in DKO mice (Fig. 3B).

Bcl6-deficient mice show altered bone parameters such as significantly decreased bone volume per tissue volume (BV/TV), trabecular thickness (Tb.Th) and trabecular number (Tb.N) as well as elevated trabecular separation (Tb.Sp). Bone morphogenetic

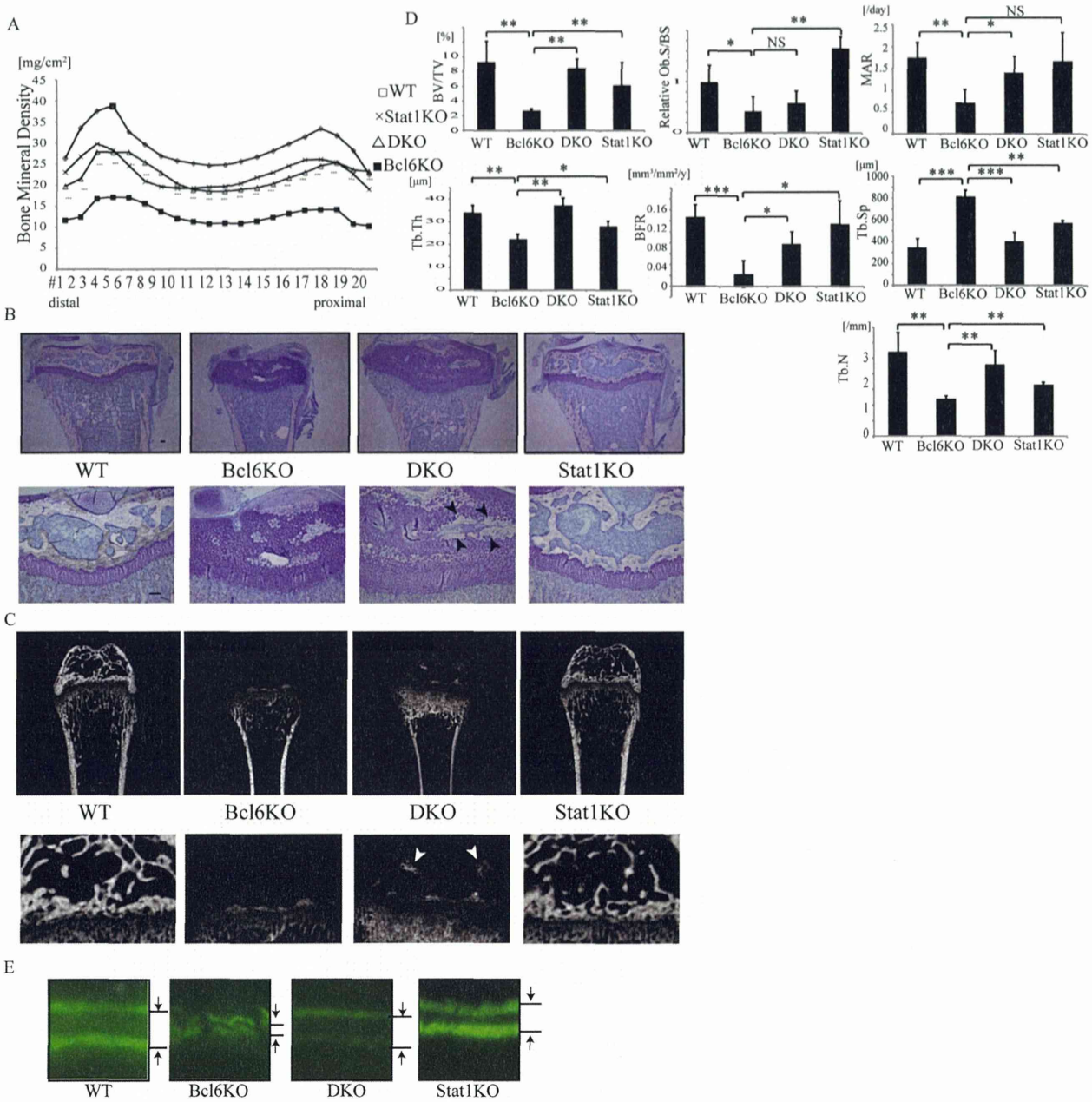

Fig. 3. Elevated Stat1 expression inhibits bone formation in Bcl6 KO mice *in vivo*. (*A*) Bone mineral density (BMD) of an equal longitudinal division of femurs from six weeks old wild-type (WT, open boxes), Bcl6 KO (Bcl6 KO, closed boxes), Stat1 KO (Stat1 KO, crosses) and Bcl6-Stat1 DKO female mice (DKO, open triangles). Data represent mean ± s.d of BMD ($n = 3$–5). (*B, C*) *Toluidine blue staining (B) and micro CT analysis (C) of WT, Bcl6 KO, Stat1 KO and DKO bones. Lower panels in B and C show higher magnification images of upper* panels. Arrowheads indicate ossification (B and C). Bar = 100 μm. (D) Bone morphogenetic analysis of six weeks old WT, Bcl6 KO, Stat1 KO and DKO female animals. Data represent means ± s.d of bone volume per tissue volume (BV/TV), trabecular thickness (Tb.Th), trabecular number (Tb.N), trabecular separation (Tb.Sp), osteoblast surface per bone surface (Ob.S/BS), mineral apposition rate (MAR) and bone formation rate (BFR) in WT, Bcl6 KO, Stat1 KO and DKO. Data represent means ± s.d (*$P < 0.05$, **$P < 0.01$, ***$P < 0.001$, NS: not significant, $n = 3$–5). (E) Representative images of calcein labeling in WT, Bcl6 KO, Stat1 KO and DKO tibia bones. Calcein was injected into peritoneal cavity of WT, Bcl6 KO, Stat1 KO or DKO mice, one and five days before sacrifice.

analysis demonstrated that altered bone volume and bone-forming parameters, such as BV/TV, Tb.Th, Tb.N, Tb.Sp, MAR and BFR, seen in Bcl6 KO mice were significantly rescued in DKO mice (Fig. 3D). Inhibited osteoblastic parameters in Bcl6-deficient compared with wild-type mice, as shown by reduced osteoblast surface per bone surface (Ob.S/BS), mineral apposition rate (MAR) and bone formation rate (BFR), were all increased in DKO mice (Fig. 3D, E). We previously showed that osteoclasts are activated in Bcl6-deficient mice [12], and it is possible that increased bone mass seen in DKO mice was due to decreased osteoclast activity. However, Stat1 deficiency also reportedly elevates osteoclast formation [13].

3.4. *Stat1 deficiency rescues altered osteoblastogenesis in Bcl6-deficient osteoblasts*

To determine if elevated bone mass and osteoblastic activity seen in DKO compared to Bcl6-deficient mice were due to increased osteoblastogenesis, we undertook *in vitro* culture of osteoblasts from wild-type (WT), Bcl6-deficient (Bcl6 KO), Stat1-deficient (Stat1 KO) or DKO mice and stimulated cells with BMP2 (Fig. 4). Osteoblastogenesis was evaluated by Alp staining and *Alp*, *Col1a1* and *Sp7* gene expression. We found that osteoblastogenesis, which was significantly inhibited in Bcl6-deficient compared with wild-type osteoblasts, was significantly restored in DKO osteoblasts (Fig. 4A, B). Stat1 reportedly attenuates osteoblastogenesis by inhibiting nuclear translocation of Runx2, which is required for osteoblast differentiation [13,24]. Indeed, immunostaining showed that nuclear translocation of Runx2 by BMP2 seen in wild-type osteoblasts was significantly inhibited in Bcl6-deficient osteoblasts but rescued in DKO mice (Fig. 4C, D).

4. Discussion

Osteoclasts and osteoblasts cooperatively regulate bone mass [2,3]. Osteoclast differentiation is promoted by stimulation with the cytokines M-CSF and RANKL, while osteoblastogenesis is activated by BMP2 or Wnt [25,26]. Various other factors are activated downstream of these regulators during cell differentiation [27,28]. Osteoclasts and osteoblasts are derived from hematopoietic and mesenchymal stem cells, respectively, and their differentiation is regulated by cell type specific regulators such as c-Fos and NFTAc1 in osteoclasts or Runx2 and Sp7 in osteoblasts [4,6,29]. However, here, we found that Bcl6, which inhibits osteoclast formation [12], promotes osteoblastogenesis. Thus, Bcl6 plays crucial roles in the differentiation of both cell types. We previously showed that Bcl6 inhibits expression of osteoclastic genes such as *NFATc1*, *Cathepsin K* and *DC-STAMP* in osteoclast progenitors [12], while the present study demonstrates that Bcl6 alters Stat1 expression in osteoblasts (Fig. 4E). Bcl6 expression was not affected by BMP2 treatment and was stable during osteoblastogenesis. Bcl6 loss in osteoblasts significantly elevated Stat1 expression, attenuating Runx2 nuclear translocation stimulated by BMP2. Thus, Bcl6 plays no role in basal osteoblastogenesis in the absence of BMP2 but rather inhibits osteoblast differentiation by attenuating Runx2 nuclear activity (Fig. 4E). We previously reported that decreased bone mass seen in Bcl6-deficient mice is due to accelerated osteoclastogenesis [12]. However, our results suggest that reduced bone mass in Bcl6-deficient mice could be due to both inhibited osteoblastic activity and accelerated osteoclast formation. To date, bone diseases such as osteoporosis have been treated with either anti-bone resorptive or bone-forming agents, and reagents regulating both cell types

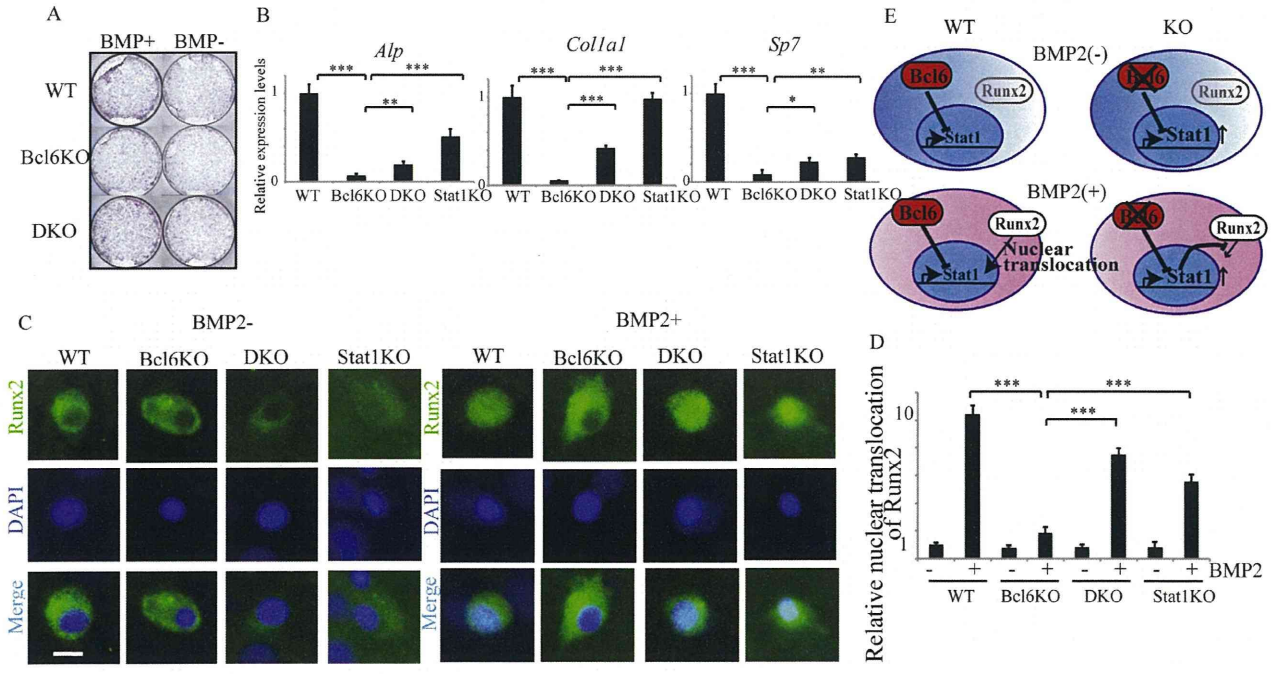

Fig. 4. Stat1 deficiency rescues inhibited osteoblastogenesis in Bcl6-deficient cells. (A, B) Primary osteoblasts were isolated from WT, Bcl6 KO, Stat1 KO and DKO mice and cultured in the presence or absence of BMP2 (300 ng/ml) for three days. Osteoblastogenesis was then evaluated by Alp staining (A) and realtime PCR for *Alp*, *Col1a1* and *Sp7* (B). Data represent means ± s.d of *Alp*/*β-actin*, *Col1a1*/*β-actin* or *Sp7*/*β-actin* levels ($^{*}P < 0.05$, $^{**}P < 0.01$, $^{***}P < 0.001$, $n = 3$). (C, D) Primary osteoblasts isolated from WT, Bcl6 KO, Stat1 KO and DKO mice were cultured with or without BMP2 (300 ng/ml) for three days, stained with anti-Runx2 antibody and DAPI and observed under a fluorescence microscope (C), and cells showing nuclear Runx2 were counted (D). Data represent relative means ± s.d. of cells exhibiting nuclear Runx2 ($^{*}P < 0.05$, $^{**}P < 0.01$, $^{***}P < 0.001$, $n = 3$). Bar = 10 μm. Representative data of two independent experiments are shown. (E) Bcl6 is required to promote osteoblastogenesis by inhibiting expression of *Stat1*, an attenuator of Runx2, a transcription factor essential for osteoblast differentiation. Bcl6 expression is stable during osteoblast differentiation and functions in osteoblastogenesis by inhibiting Stat1 expression at a time when Runx2 nuclear translocation is stimulated by BMP2.

concomitantly to increase bone mass have been sought. Interestingly, recent studies report several molecules that regulate both osteoclasts and osteoblasts [14,15,17], and here we demonstrate that Bcl6 could serve as a target to increase bone mass by both inhibiting osteoclasts and activating osteoblasts. Since deregulated Bcl6 expression reportedly promotes multiple myeloma cell growth [30], Stat1 inhibition could be a better option to activate osteoblasts in bones. Currently, a Stat1 inhibitor is being assessed to treat hematologic malignancies [31].

Runx2 is required to promote osteoblast differentiation, and Runx2-deficient mice show complete lack of bone formation leading to peri-neonatal lethality [4]. We demonstrated here that Bcl6 directly regulates expression of Stat1, an attenuator of Runx2, in osteoblasts, and that lack of Bcl6 significantly elevates Stat1 levels; however, Bcl6-deficient mice did not exhibit peri-neonatal lethality, although bone formation was severely altered. These results suggest that the Bcl6-Stat1 axis is not the sole system regulating Runx2 function. In addition, some phenotypes observed in Bcl6-deficient mice were fully restored by Stat1 deletion, while others were not or were only partially rescued, suggesting that Bcl6 and Stat1 may also have independent activities. Furthermore, Stat1 deletion in a Bcl6 KO background results in more moderate rescue of Bcl6 KO-associated phenotypes *in vitro* than it does in *in vivo*, suggesting that the Bcl6-Stat1 axis likely plays both direct and indirect roles in regulating osteoblastogenesis. Further studies are needed to determine how osteoblast differentiation is regulated by Bcl6 and Stat1.

Since osteoblast activity is coupled with osteoclastic activity, severe inhibition of osteoclasts by reagents such as bisphosphonate also alters osteoblast activity. Although, the number of patients diagnosed was small, some investigators report that inhibition of bone turnover beyond physiological levels promotes development of osteonecrosis of the jaws and severely suppressed bone turnover (SSBT) [32,33]. Osteoclastogenesis is reportedly activated in either Bcl6- or Stat1-deficient mice, as observed by our group or others, respectively [12,13]. However, we found that DKO mice exhibited higher bone mass compared with Bcl6-deficient mice (Fig. 3). The net increase in bone mass seen in DKO mice suggests that Stat1 inhibition is dominant over activation of osteoclasts and that Stat1 could be a therapeutic target to increase bone mass without inhibiting bone turnover, even under conditions of osteoclast activation.

Conflict of interest

The authors have no conflicting financial interests.

Acknowledgments

T. Miyamoto was supported by a Grant-in-aid for Scientific Research, Japan.

Transparency document

The transparency document associated with this article can be found in the online version at http://dx.doi.org/10.1016/j.bbrc.2015.01.012.

Appendix A. Supplementary data

Supplementary data related to this article can be found at http://dx.doi.org/10.1016/j.bbrc.2015.01.012.

References

[1] T.J. Martin, N.A. Sims, Osteoclast-derived activity in the coupling of bone formation to resorption, Trends Mol. Med. 11 (2) (2005) 76–81.
[2] T.D. Rachner, S. Khosla, L.C. Hofbauer, Osteoporosis: now and future, Lancet 377 (2011) 1276–1287.
[3] E. Seeman, P.D. Delmas, Bone quality – the material and structural basis of bone strength and fragility, N. Engl. J. Med. 354 (2006) 2250–2261.
[4] T. Komori, H. Yagi, S. Nomura, et al., Targeted disruption of Cbfa1 results in a complete lack of bone formation owing to maturational arrest of osteoblasts, Cell 89 (5) (1997) 755–764.
[5] P. Ducy, R. Zhang, V. Geoffroy, et al., Osf2/Cbfa1: a transcriptional activator of osteoblast differentiation, Cell 89 (5) (1997) 747–754.
[6] K. Nakashima, X. Zhou, G. Kunkei, et al., The novel zinc finger-containing transcription factor osterix is required for osteoblast differentiation and bone formation, Cell. 108 (1) (2002) 17–29.
[7] H. Takayanagi, S. Kim, T. Koga, et al., Induction and activation of the transcription factor NFATc1(NFATc2) integrate RANKL signaling in terminal differentiation of osteoclasts, Dev. Cell 3 (2002) 889–901.
[8] A.E. Grigoriadis, Z.Q. Wang, M.G. Cecchini, et al., c-Fos: a key regulator of osteoclast-macrophage lineage determination and bone remodeling, Science 266 (5184) (1994) 443–448.
[9] K. Matsuo, D.L. Galson, C. Zhao, et al., Nuclear factor of activated T-cells (NFAT) rescues osteoclastogenesis in precursors lacking c-Fos, J. Biochem. 279 (25) (2004) 26475–26480.
[10] C. Bastard, H. Tilly, B. Lenormand, et al., Translocations involving band 3q27 and Ig gene regions in non-Hodgkin's lymphoma, Blood 79 (1992) 2527–2531.
[11] H. Ohno, Pathogenetic and clinical implications of non-immunoglobulin; Bcl6 translocations in B-cell non-Hodgkin's lymphoma, J. Clin. Exp. Hematop. 46 (2) (2006) 43–53.
[12] Y. Miyauchi, K. Ninomiya, H. Miyamoto, et al., The Blimp1-Bcl6 axis is critical to regulate osteoclast differentiation and bone homeostasis, J. Exp. Med. 207 (4) (2010) 751–762.
[13] S. Kim, T. Koga, M. Isobe, et al., Stat1 functions as cytoplasmic attenuator of Runx2 in the transcriptional program of osteoblast differentiation, Genes Dev. 17 (16) (2003) 1979–1991.
[14] M. Hayashi, T. Nakashima, M. Taniguchi, et al., Osteoprotection by semaphoring 3A, Nature 485 (7396) (2012) 69–74.
[15] R. Kiviranta, K. Yamana, H. Saito, et al., Coordinated transcriptional regulation of bone homeostasis by Ebf1 and Zfp521 in both mesenchymal and hematopietic lineages, J. Exp. Med. 210 (5) (2013) 969–985.
[16] M. Yagi, T. Miyamoto, Y. Sawatani, et al., DC-STAMP is essential for cell-cell fusion in osteoclasts and foreign body giant cells, J. Exp. Med. 202 (3) (2005) 34–51.
[17] S.H. Lee, J. Rho, D. Jeong, et al., v-ATPase V0 subunit d2-deficient mice exhibit impaired osteoclast fusion and increased bone formation, Nat. Med. 12 (12) (2006) 1403–1409.
[18] T. Fukuda, T. Yoshida, S. Okada, et al., Disruption of Bcl6 gene results in an impaired germinal center formation, J. Exp. Med. 186 (3) (1997) 439–448.
[19] M.A. Meraz, J.M. White, K.C.F. Sheehan, et al., Targeted disruption of the Stat1 gene in mice reveals unexpected physiologic specificity in the JAK-STAT signaling pathway, Cell 84 (3) (1996) 431–442.
[20] Y. Miyauchi, Y. Sato, T. Kobayashi, et al., HIF1α is required for osteoclast activation by estrogen deficiency in postmenopausal osteoporosis, Proc. Natl. Acad. Sci. U. S. A. 110 (41) (2013) 16568–16573.
[21] J.M. Polo, P. Juszczynski, S. Monti, et al., Transcriptional signature with differential expression of Bcl6 target genes accurately identifies Bcl6-dependent diffuse large B cell lymphomas, Proc. Natl. Acad. Sci. U. S. A. 104 (9) (2007) 3207–3212.
[22] C.H. Heldin, K. Miyazono, P. Dijke, TGF-β signaling from cell membrane to nucleus through SMAD proteins, Nature 390 (6659) (1997) 465–471.
[23] Y. Yoshida, S. Tanaka, H. Umemori, et al., Negative regulation of BMP/Smad signaling by Tob in osteoblasts, Cell. 103 (7) (2000) 1085–1097.
[24] H. Takayanagi, S. Kim, T. Koga, et al., Stat1-mediated cytoplasmic attenuation in osteoimmunology, J. Cell. Biochem. 94 (2) (2005) 232–240.
[25] E.A. Wang, V. Rosen, J.S. D'alessandro, et al., Recombinant human bone morphogenetic protein induces bone formation, Proc. Natl. Acad. Sci. U. S. A. 87 (1990) 2220–2224.
[26] E. Canalis, Wnt singaling in osteoporosis:mechanisms and novel therapeutic approaches, Nat. Rev. Endocrinol. 9 (10) (2013) 575–583.
[27] E.M. Lewiecki, New targets for intervention in the treatment of postmenopausal osteoporosis, Nat. Rev. Rheumatol. 7 (11) (2011) 631–638.
[28] H. Takayanagi, Osteoimmunology: shared mechanisms and crosstalk between the immune and bone systems, Nat. Rev. Immunol. 7 (4) (2007) 292–304.
[29] S.L. Teitelbaum, F.P. Ross, Genetic regulation of osteoclast development and function, Nat. Rev. Genet. 4 (8) (2003) 638–649.
[30] T. Hideshima, C. Mitsiades, H. Ikeda, et al., A proto-oncogene BCL6 is up-regulated in the bone marrow microenvironment in multiple myeloma cells, Blood 115 (18) (2010) 3772–3775.
[31] D.A. Frank, S. Mahajan, J. Ritz, Fludarabine-induced immunosuppression is associated with inhibition of STAT1 signaling, Nat. Med. 5 (4) (1999) 444–447.
[32] C.V. Obvina, J.E. Zerwekh, D.S. Rao, et al., Severely suppressed bone turnover: a potential complication of alendronate therapy, J. Clin. Endocrinol. Metab. 90 (3) (2005) 1294–1301.
[33] G.A. Rodan, T.J. Martin, Therapeutic approaches to bone disease, Science 289 (5484) (2000) 1508–1514.

THE JOURNAL OF BIOLOGICAL CHEMISTRY VOL. 290, NO. 2, pp. 716–726, January 9, 2015
© 2015 by The American Society for Biochemistry and Molecular Biology, Inc. Published in the U.S.A.

Interleukin-1 Receptor-associated Kinase-4 (IRAK4) Promotes Inflammatory Osteolysis by Activating Osteoclasts and Inhibiting Formation of Foreign Body Giant Cells*

Received for publication, March 25, 2014, and in revised form, November 12, 2014 Published, JBC Papers in Press, November 17, 2014, DOI 10.1074/jbc.M114.568360

Eri Katsuyama[‡1], Hiroya Miyamoto[‡1], Tami Kobayashi[‡§], Yuiko Sato[‡¶], Wu Hao[‡], Hiroya Kanagawa[‡], Atsuhiro Fujie[‡], Toshimi Tando[‡], Ryuichi Watanabe[‡], Mayu Morita[‖], Kana Miyamoto[‡], Yasuo Niki[‡1], Hideo Morioka[‡], Morio Matsumoto[‡], Yoshiaki Toyama[‡], and Takeshi Miyamoto[‡§2]

From the Departments of [‡]Orthopedic Surgery, [§]Integrated Bone Metabolism and Immunology, [¶]Musculoskeletal Reconstruction and Regeneration Surgery, and [‖]Dentistry and Oral Surgery, Keio University School of Medicine, 35 Shinano-machi, Shinjuku-ku, Tokyo 160-8582, Japan

Background: Currently, it is not clear how osteoclasts and foreign body giant cells (FBGCs) are differentially regulated.
Results: Inflammatory cytokines and infection mimetics activated osteoclastogenesis and inhibited FBGC formation, as indicated by M1/M2 macrophage polarization, in an IRAK4-dependent manner.
Conclusion: Osteoclasts and FBGCs are reciprocally regulated by IRAK4.
Significance: This study provides a basis for understanding regulation of foreign body reactions via IRAK4.

Formation of foreign body giant cells (FBGCs) occurs following implantation of medical devices such as artificial joints and is implicated in implant failure associated with inflammation or microbial infection. Two major macrophage subpopulations, M1 and M2, play different roles in inflammation and wound healing, respectively. Therefore, M1/M2 polarization is crucial for the development of various inflammation-related diseases. Here, we show that FBGCs do not resorb bone but rather express M2 macrophage-like wound healing and inflammation-terminating molecules *in vitro*. We also found that FBGC formation was significantly inhibited by inflammatory cytokines or infection mimetics *in vitro*. Interleukin-1 receptor-associated kinase-4 (IRAK4) deficiency did not alter osteoclast formation *in vitro*, and IRAK4-deficient mice showed normal bone mineral density *in vivo*. However, IRAK4-deficient mice were protected from excessive osteoclastogenesis induced by IL-1β *in vitro* or by LPS, an infection mimetic of Gram-negative bacteria, *in vivo*. Furthermore, IRAK4 deficiency restored FBGC formation and expression of M2 macrophage markers inhibited by inflammatory cytokines *in vitro* or by LPS *in vivo*. Our results demonstrate that osteoclasts and FBGCs are reciprocally regulated and identify IRAK4 as a potential therapeutic target to inhibit stimulated osteoclastogenesis and rescue inhibited FBGC formation under inflammatory and infectious conditions without altering physiological bone resorption.

Biomaterial implants, including pacemakers, artificial joints, prostheses, dental implants, and bone devices, are now necessities of human life. Indeed, it is estimated that 20–25 million people in the United States have some type of implanted medical device (1). Inflammation and infection are primary factors underlying implant failure (2, 3), often with disastrous consequences for device function and the patient. Thus preventing these failures is crucial for patients' well being.

A foreign body response (FBR)[3] characterized by foreign body giant cell (FBGC) formation occasionally occurs following implantation of foreign materials (4). FBGC formation emerging from implanted biomaterials is reportedly associated with biomaterial degradation and failure (5–7); thus, controlling FBGC formation is considered critical to prevent implant failure. Nonetheless, we have little understanding of mechanisms underlying the FBR or how FBGC differentiation is regulated.

FBGCs are formed by cell-cell fusion of mononuclear cells (8–10). Various molecules, such as dendritic cell-specific transmembrane protein (DC-STAMP), ATPv0d2, MFR, CD47, CD44, DAP12, and OC-STAMP reportedly function in macrophage fusion (9, 11–17). Osteoclasts are also multinuclear giant cells derived from monocyte/macrophage lineage cells, and their multinucleation is also induced by fusion of mononuclear osteoclasts. Although both FBGC and osteoclast formation are induced by fusion of mononuclear cells in a DC-STAMP-dependent manner, regulation of FBGC and osteoclast differentiation likely differs. Indeed, we have previously reported that transcription of *DC-STAMP* is regulated differently in osteoclasts than it is in FBGCs (10). Therefore, we hypothesize that FBGCs play a role in FBR different from osteoclasts.

Osteoclasts play a critical role in bone resorption, destruction, and osteolysis. In addition, inhibition of osteoclast differentiation and function is considered crucial to prevent bone loss and osteolysis-induced implant failure (18, 19). However, strong osteoclast inhibition beyond levels required for physio-

* This work was supported by a grant-in-aid for scientific research.
[1] These authors contributed equally to this work.
[2] To whom correspondence should be addressed: Dept. of Orthopedic Surgery, Keio University School of Medicine, 35 Shinano-machi, Shinjuku-ku, Tokyo 160-8582, Japan. Tel.: 81-3-5363-3812; Fax: 81-3-3353-6597; E-mail: miyamoto@z5.keio.jp.

[3] The abbreviations used are: FBR, foreign body response; FBGC, foreign body giant cell; DC-STAMP, dendritic cell-specific transmembrane protein; RANKL, nuclear factor κ-B ligand; TRAP, tartrate-resistant acid phosphatase; BS, bone surface; OC, osteoclast surface; PVA, polyvinyl alcohol; BMD, bone mineral density.

Downloaded from http://www.jbc.org/ at Keio University Shinanomachi Media Center on February 25, 2015

logical bone metabolism frequently causes adverse effects such as osteopetrosis, osteonecrosis, or severely suppressed bone turnover (20–23). Thus, specific inhibitors of pathologically activated osteoclast levels resulting from inflammation or infection have been sought.

Macrophages consist of two major subpopulations, M1 and M2 (24, 25). M1 macrophages are activated by various stimuli, including bacterial or viral infections, and express inflammatory cytokines. In contrast, M2 macrophages function in parasitic infections, allergic responses, or wound healing (26). Thus, M1/M2 polarization status is considered crucial for the development of various diseases (27).

Interleukin-1 receptor-associated kinase-4 (IRAK4) is a member of the interleukin-1 receptor-associated kinase family of proteins composed of IRAK1–4. Interleukin-1 receptor-associated kinases transduce inflammatory cytokine and toll-like receptor signals and reportedly function in the activation of natural killer cells, antigen-presenting cells, and T cells (28–31). IRAK4 is reported to play a role in regulating both IL-1 and toll-like receptor signaling (28).

Here, we report two critical findings that strongly suggest that implant failure due to bone loss likely results from activity of osteoclasts rather than FBGCs. First, we show that FBGCs, unlike osteoclasts, cannot resorb bone but rather express wound-healing and inflammation-terminating molecules, such as Ym1 and Alox15. Second, promotion of bone loss and inhibition of FBGC formation by LPS seen in wild-type mice were both completely abrogated in mice deficient in IRAK4. Furthermore, loss of IRAK4 *in vitro* and *in vivo* did not inhibit physiological osteoclastogenesis, and IRAK4-deficient mice exhibited normal bone mass. Overall, our findings show that FBGC and osteoclast differentiation are reciprocally regulated by IRAK4 and suggest that targeting IRAK4 could antagonize implant failure by promoting FBGC formation and blocking osteoclastogenesis.

EXPERIMENTAL PROCEDURES

Mice—IRAK4-deficient mice were provided by the Department of Medical Biophysics, Ontario Cancer Institute. Wild-type mice on a C57BL/6 background were purchased from Sankyo Lab (Tsuchiura, Japan). Animals were maintained under specific pathogen-free conditions in animal facilities certified by the animal care committee at the Keio University School of Medicine. Animal protocols were approved by the animal care committee at the Keio University School of Medicine.

Reagents—Macrophage colony-stimulating factor (M-CSF), GM-CSF, IL-4, and IL-1β were purchased from R&D Systems (Minneapolis, MN). Recombinant soluble receptor activator of nuclear factor κ-B ligand (RANKL) was purchased from PeproTech Ltd. (Rocky Hill, NJ). LPS and zymosan were purchased from Sigma.

In Vitro Osteoclastogenesis Assay—Bone marrow cells were isolated from wild-type or IRAK4-deficient mice and cultured in α-modified Eagle's minimum essential medium (Sigma) containing 10% heat-inactivated FBS (JRH Biosciences, Lenexa, KS) and GlutaMAX (Invitrogen) supplemented with 50 ng/ml M-CSF for 3 days. M-CSF-dependent adherent cells were then harvested as osteoclast and FBGC common progenitors, and 5×10^4 cells were plated in each well of 96-well culture plates. Cells were cultured with M-CSF (50 ng/ml) or M-CSF (50 ng/ml) plus RANKL (25 ng/ml) with or without IL-1β (10 ng/ml) for 2–6 days. Osteoclastogenesis was evaluated by tartrate-resistant acid phosphatase (TRAP) and May-Grünwald Giemsa staining (9, 32). Multinuclear cells containing more than 3 or 10 nuclei were scored as osteoclasts. Total RNAs were isolated from osteoclasts using an RNeasy mini kit (Qiagen, Hilden, Germany).

For the pit formation assay, osteoclast progenitors were cultured on dentine slices in the presence of M-CSF plus RANKL for 10–12 days (33). Resorbing lacunae were visualized by toluidine blue staining, and the relative resorbing area was scored under a microscope (BZ-9000, Keyence Co., Tokyo, Japan).

For the osteoclast survival assay, wild-type or IRAK4-deficient osteoclasts induced in the presence of M-CSF plus RANKL with or without IL-1β were stained with TRAP at time 0 or were washed three times with PBS, then cultured in cytokine-free media for 3 more hours, and stained with TRAP. Multinuclear TRAP-positive cells were scored as surviving cells.

In Vitro Foreign Body Giant Cell Formation Assay—M-CSF-dependent osteoclasts and FBGC common progenitor cells were harvested as above, and 5×10^4 cells were plated in each well of 96-well culture plates. Cells were cultured in α-modified Eagle's minimum essential medium containing 10% FBS in the presence of GM-CSF (50 ng/ml) plus IL-4 (50 ng/ml) with or without the indicated concentrations of IL-1β, LPS, or zymosan for 2–4 days. Cells were then stained with May-Grünwald Giemsa (10) and observed under a microscope (BZ-9000, Keyence Co., Tokyo, Japan). Multinuclear cells containing more than three nuclei were scored as FBGCs. Total RNAs were isolated from FBGCs using an RNeasy mini kit (Qiagen, Hilden, Germany).

Analysis of Bone Mineral Density (BMD)—Eight-week-old male wild-type or IRAK4-deficient mice were necropsied, and their hindlimbs were removed, fixed with 70% ethanol, and subjected to dual energy x-ray absorptiometric scan analysis to measure BMD (mg/cm^2), using a DCS-600R system (Aloka Co. Ltd, Tokyo, Japan).

Analysis of Skeletal Morphology—Eight-week-old female wild-type and IRAK4-deficient mice were administered intraperitoneal injections of 10 mg/kg calcein (Dojindo Co.) at 5 days and 1 day before sacrifice to evaluate bone formation rate. Left hindlimbs were removed and fixed with 70% ethanol, and undecalcified bones were embedded in glycol methacrylate. Sections of 3 μm were cut longitudinally in the proximal region of the tibia and stained with toluidine blue O. Histomorphometric measurement was performed in stained sections from the secondary spongiosa area 1.05 mm from the growth plate and 0.4 mm from the end of metaphysis using OsteoMeasure software (OsteoMetrics, Inc. Decatur, GA).

Analysis of Osteolysis in the Murine Calvarium—Wild-type or IRAK4-deficient mice were anesthetized with ketamine. A region of skin overlying the skull was shaved, and 100 μl of PBS containing LPS (50 mg/kg) was injected onto the periosteal surface of calvariae. Five days later, mice were euthanized, and calvariae were harvested for RNA isolation or a micro-com-

Downloaded from http://www.jbc.org/ at Keio University Shinanomachi Media Center on February 25, 2015

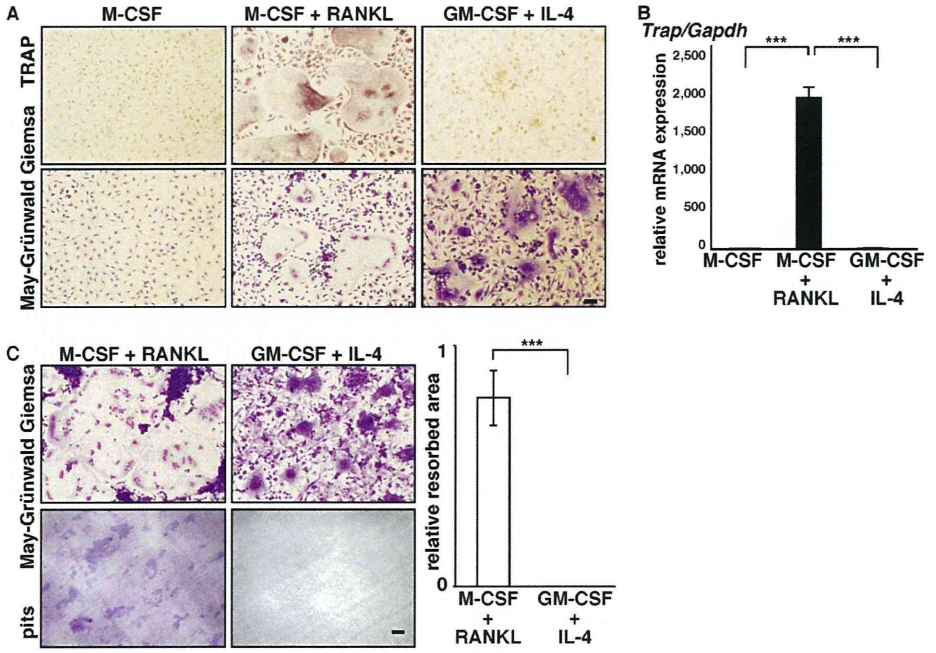

FIGURE 1. **FBGCs fail to resorb bone.** *A* and *B*, osteoclast and FBGC common progenitor cells were cultured in the presence of M-CSF plus RANKL (for osteoclasts) or GM-CSF plus IL-4 (for FBGCs), and cells were subjected to TRAP and May-Grünwald Giemsa staining (*bar* = 100 μm) (*A*), a real time PCR assay for *Trap* expression relative to *Gapdh* (*B*), or May-Grünwald Giemsa staining and a bone resorption assay on dentine slices (*bar*, 100 μm) (*C*). Data represent means ± S.D of *Trap/Gapdh* levels (***, $p < 0.001$; $n = 3$). Resorbing lacunae were visualized by toluidine blue staining (*C, left panel*), and the relative area resorbed was quantified. Data represent means ± S.D of the resorbed area in FBGC relative to osteoclast samples (***, $p < 0.001$; $n = 3$) (*C, right panel*). Shown are representative data of at least three independent experiments.

puted tomography scan (R_mCT2; Rigaku Corp., Tokyo, Japan). Scanning was conducted at 90 kV and 160 μA. A three-dimensional region of interest was created at the level of the parietal bones. Osteoclast formation in calvariae was evaluated by TRAP staining or immunofluorescence staining for cathepsin K. For TRAP stain, the calvarial bone was fixed in 4% paraformaldehyde overnight at 4 °C with gentle shaking. After washing with PBS, sections were stained with TRAP. For cathepsin K staining, calvariae were fixed in 10% neutral-buffered formalin, decalcified in 10% EDTA (pH 7.4), embedded in paraffin, and cut into 4-μm sections. After microwave treatment for 10 min in 1 mM EDTA (pH 6.0) for antigen retrieval followed by blocking with 5% BSA/PBS for 60 min, sections were stained with anti-cathepsin K (Ctsk) (ab19027, 1:100 dilution; Abcam, Cambridge, UK) or ISO-type control antibody (3900, 1:100 dilution; Cell Signaling) overnight at 4 °C. After washing in PBS, sections were stained with Alexa Fluor 488/goat anti-rabbit IgG (1:200 dilution; Invitrogen) for 1 h at room temperature. DAPI (1:2000; Wako Pure Chemicals Industries, Osaka, Japan) served as a nuclear stain. A fluorescence microscope (Biorevo; Keyence, Osaka, Japan) was used to examine immunostained sections.

In Vivo FBGC Formation Assay—Wild-type or IRAK4-deficient mice were anesthetized with ketamine, and polyvinyl alcohol (PVA) sponges (10 × 10 × 0.5 mm) containing either PBS or LPS (25 mg/kg) were implanted into the intraperitoneal space, as described previously (17). Six days later, sponges were harvested, and histological analyses were performed using hematoxylin and eosin (H&E) staining. Multinuclear cells that contained more than three nuclei and adhered to implants were scored as FBGCs. Total RNAs were isolated from sponges using TRIzol reagent (Invitrogen).

Real Time PCR Analysis—Total RNAs were isolated from macrophages, osteoclasts, FBGCs, calvaria or PVA sponges, and single-stranded complementary DNAs (cDNAs) were synthesized with reverse transcriptase (Clontech). Real time PCR was performed using SYBR Premix ExTaq II (Takara Bio Inc., Otsu, Shiga, Japan) with a DICE Thermal cycler (Takara Bio Inc.), according to the manufacturer's instructions. β-Actin or *Gapdh* expression served as internal controls for real time PCR. Primers for β-actin, *Ctsk*, and *DC-stamp* were described previously (34). Other primer sequences were as follows: *TNF-α*-forward, 5′-AAGCCTGTAGCCCACGTCGTA-3′, and *TNF-α*-reverse, 5′-GGCACCACTAGTTGGTTGTCTTTG-3′; *Ym1*-forward, 5′-TTTGATGGCCTCAACCTGGA-3′, and *Ym1*-reverse, 5′-AGTGAGTAGCAGCCTTGGAATGTC-3′; *Alox15*-forward, 5′-TGAAGCGGTCTACTTGTCTCCCTG-3′, and *Alox15*-reverse, 5′-AAGGAAGAAATCCGCTTCAA-ACAG-3′; *Trap*-forward, 5′-TTGCGACCATTGTTAGCCA-CATA-3′, and *Trap*-reverse, 5′-TCAGATCCATAGTGAAA-CCGCAAG-3′; *Gapdh*-forward, 5′-AGCCTCGTCCCGTAG-ACAAAAT-3′, and *Gapdh*-reverse, 5′-ATGGCAACAATCT-CCACTTTGC-3′; *Fizz1*-forward, 5′-GACTATGAACAGAT-GGGCCTCCT-3′, and *Fizz1*-reverse, 5′-GTCAACGAGTAA-GCACAGGCAGT-3′; *CD206*-forward, 5′-ACCTGGCAAGT-ATCCACAGCATT-3′, and *CD206*-reverse, 5′-AATGTCAC-TGGGGTTCCATCACT-3′; ariginase1-forward, 5′-TTAGA-GATTATCGGAGCGCCTTTC-3′, and ariginase1-reverse, 5′-CCGTGGTCTCTCACGTCATACTCT-3′; *Rankl*-forward, 5′-CAATGGCTGGCTTGGTTTCATAG-3′, and *Rankl*-

Downloaded from http://www.jbc.org/ at Keio University Shinanomachi Media Center on February 25, 2015

reverse, 5′-CTGAACCAGACATGACAGCAGCTGGA-3′; *IL-12*-forward, 5′-ACCTGCTGAAGACCACAGATGAC-3′, and *IL-12*-reverse, 5′-GTCTTCAATGTGCTGGTTTGGTC-3′; *Nos2*-forward, 5′-AGAAAACCCCTTGTGCTGTTCTC-3′, and *Nos2*-reverse, 5′-CAGGGATTCTGGAACATTCTGTG-3′.

Western Blot Analysis—Whole cell lysates were prepared from bone marrow cultures using RIPA buffer (1% Tween 20, 0.1% SDS, 150 mM NaCl, 10 mM Tris-HCl (pH 7.4), 0.25 mM phenylmethylsulfonyl fluoride, 10 μg/ml aprotinin, 10 μg/ml leupeptin, 1 mM Na_3VO_4, 5 mM NaF (Sigma)). Cell lysates were collected after 10 min of centrifugation at 15,000 rpm at 4 °C. Equivalent amounts of protein were separated by SDS-PAGE and transferred to a PVDF membrane (Millipore Corp.). Proteins were detected using the following antibodies: anti-Ym1 (ab93034, Abcam); anti-Alox15 (ab80221, Abcam); anti-phospho-p38 MAPK (9211, Cell Signaling); anti-p38 MAPK (9212, Cell Signaling); anti-phospho-p44/42 MAPK (9106, Cell Signaling); anti-p44/42 MAPK (9102, Cell Signaling); anti-phospho-SAPK/JNK (9255, Cell Signaling); anti-SAPK/JNK (9252, Cell Signaling); anti-actin (A2066, Sigma); and isotype control (ab171870, Abcam). Bands were quantified as described (35).

Statistical Analyses—Statistical analyses were performed using the unpaired two-tailed Student's *t* test (*, $p < 0.05$; **, $p < 0.01$; ***, $p < 0.001$; NS, not significant, throughout the paper). All data are expressed as the mean ± S.D.

RESULTS

FBGCs Fail to Resorb Bone—Osteoclasts and FBGCs differentiate from common myeloid lineage precursor cells, and both form multinuclear cells by fusion (9, 17). However, we found that FBGCs were negative for TRAP, an osteoclast marker (Fig. 1*A*). We also found that normalized to *Gapdh* or β-actin, *Trap* mRNA expression was significantly lower in FBGCs than in osteoclasts (Fig. 1*B* and data not shown), as described recently (36). Thus, to assess FBGC function in bone loss, we analyzed FBGC bone resorption activity using a pit formation assay (Fig. 1*C*). Osteoclast and FBGC common progenitor cells were cultured on dentine slices in the presence of M-CSF and RANKL to promote an osteoclast fate or GM-CSF plus IL-4 to produce FBGCs. Samples were then stained with toluidine blue to visualize resorbing pits on slices, and the resorbing area was quantified. FBGCs completely failed to resorb bone (Fig. 1*C*).

Inflammatory Cytokine, IL-1β, and Infection Mimetics, LPS or Zymosan, Inhibit FBGC Formation in Vitro—Because device failure is frequently associated with inflammation and infection (2, 3, 37), we asked whether FBGC differentiation is stimulated by inflammatory cytokines or infections. To do so, we treated FBGCs grown in culture with the inflammatory cytokine IL-1β, which is reportedly expressed at the FBR site (38), or with components of the bacterial or yeast cell wall, LPS, or zymosan, respectively (Fig. 2). Interestingly, multinuclear FBGC formation was significantly inhibited in the presence of IL-1β dose-dependently (Fig. 2, *A* and *B*). Expression of *DC-STAMP*, a factor essential for cell-cell fusion of either osteoclasts or FBGCs (9), was also significantly inhibited in FBGCs treated with IL-1β (Fig. 2*C*). Multinuclear FBGC formation and FBGC *DC-STAMP* expression were also significantly inhibited by LPS or zymosan, dose-dependently (Fig. 2, *D–F*). These findings strongly suggest

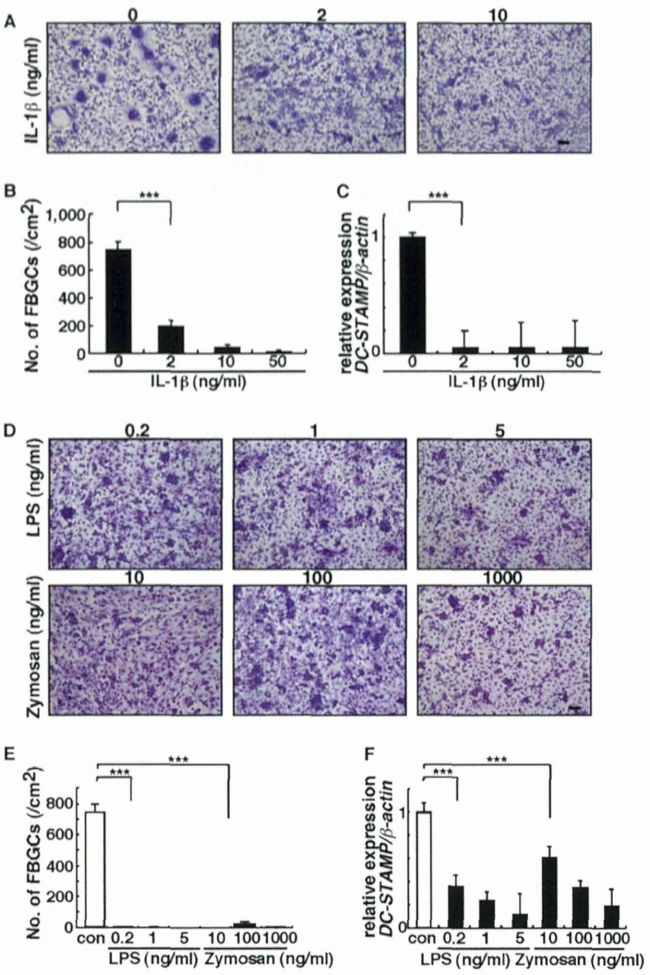

FIGURE 2. **Inflammation and infection inhibit FBGC formation.** *A*, *B*, *D*, and *E*, osteoclast and FBGC progenitor cells were cultured in the presence of GM-CSF plus IL-4 with or without indicated concentrations of IL-1β, LPS, or zymosan for 5 days, stained with May-Grünwald Giemsa (*bar*, 100 μm) (*A* and *D*), and scored for the number of multinuclear FBGCs containing more than three nuclei (***, $p < 0.001$; $n = 3$) (*B* and *E*). Representative data of at least three independent experiments are shown. *C* and *F*, total RNAs were prepared from FBGCs treated with or without indicated concentrations of IL-1β, LPS, or zymosan, and *DC-STAMP* expression relative to β-actin was analyzed by quantitative real time PCR. Data represent means ± S.D. of *DC-STAMP*/β-actin levels (***, $p < 0.001$; $n = 3$). Representative data of at least three independent experiments are shown. *con*, control.

that FBGC formation is inhibited under inflammatory or infectious conditions.

To further assess FBGC function in the FBR, we analyzed expression of chitinase-like 3 (*Ym1*) and arachidonate 15-lipoxygenase (*Alox15*) in FBGCs, macrophages, and osteoclasts by real time PCR (Fig. 3*A*). *Ym1* is a known M2 macrophage marker, and *ALOX15* encodes an enzyme functioning in wound healing and termination of inflammation (39–43). Interestingly, expression levels of both transcripts in FBGCs were significantly higher than those in macrophages and osteoclasts. Similarly, relative to *Gapdh* or β-actin, transcript levels of other M2 macrophage markers such as *Fizz1*, *CD206*, and ariginase1 were significantly higher in FBGCs than in osteoclasts (Fig. 3*A* and data not shown). Western blot analysis also indicated high expression of Ym1 and Alox15 proteins in FBGCs relative to osteoclasts; ISO-type control antibody showed no bands the

Downloaded from http://www.jbc.org/ at Keio University Shinanomachi Media Center on February 25, 2015